EXPERIMENT NO. 5

# INVESTIGATION OF THE STRUCTURAL INTEGRITY OF POLYMER BONDED EXPLOSIVES USING MECHANICAL MATERIAL TESTING

Submitted by:

Kush Jani

AEROSPACE AND OCEAN ENGINEERING DEPARTMENT

VIRGINIA POLYTECHNIC INSTITUTE AND STATE UNIVERSITY

BLACKSBURG, VIRGINIA

1 MAY 2025

EXPERIMENT PERFORMED 24 APRIL 2025

LAB TEACHING ASSISTANT: HEEJIN KIM

# MATERIALS TESTING

Kush Jani[1]
*Virginia Tech, Blacksburg, VA 24060*

## I. Introduction

The aims of this study are:

1. To characterize the fundamental mechanical properties of mock Polymer Bonded Explosive (PBX) samples, specifically the tensile modulus and compressive modulus as well as the strengths, fracture toughness, and impact energy absorption.
2. To determine and compare the modulus and strength for both sample varieties.
3. To quantify and compare the mode I fracture toughness using data from compact tension tests performed on multiple samples of each material variety.
4. To measure and compare the energy absorbed during Charpy impact testing for the neat and CNT-reinforced samples (carbon nanotube reinforced materials).

In order to meet these goals set out for this experiment, a series of mechanical tests on prepared samples of mock PBX materials with varying sugar concentrations were performed. Specifically, using an Instron Universal Testing Machine (UTM), tests for compression, tension, and fracture toughness (compact tension) were conducted via the ability of the UTM to measure load and crosshead displacement data. Furthermore, Charpy impact tests were also performed via the use of an Instron CEAST 9050 impact frame in order to measure the the energy absorbed during the fracture of samples that were notched prior during their fabrication. Through the use of these machines, the calculation of stress, strain, ultimate strength, and critical stress intensity factor as well as absorbed impact energy can be performed and further comparison of the results from said calculations would enable the direct comparison of effects on nanoparticulate presence for mechanical/material properties of PBXs.

Due to the safety concerns behind PBXs caused by their volatility, mock energetic composites were used for this investigation. Specifically, the polymer part of the PBXs was epoxy while the energetic component was ammonium perchlorate at a 3:2 ratio for AP to epoxy (Borgoltz and Talluru, 2025). The two variety of samples/materials tested in this investigation were a “neat” variant with epoxy and AP in the ratio mentioned as well as a CNT variant with 1% CNT nanoparticles by weight atop epoxy and AP (Borgoltz and Talluru, 2025). For each of these two variants, samples came in 4 different geometric variants for the 4 different tests: tension, compression, fracture toughness, and impact/charpy. The varying shapes of these samples can be seen in Figure 1.

In order to collect the needed calculations and gain a complete understanding of the material properties and differentiations in material properties for the varying samples under different tests, a background in mathematical understanding of the tests is useful and relevant. Firstly, for both the tension testing and compression testing, the equipment used will allow for the generation of displacement versus time information which will then be used to tabulate the strain and stress data for the tests, which further allows for the creation of stress versus strain diagrams. This is because the calculation of strain is based on the equation

$$\varepsilon = \frac{\Delta l}{l_0} \tag{1}$$

where $\Delta l$ is the displacement measured by the UTM for the crosshead and $l_0$ is the dimension of the sample along the axis of motion. Furthermore, the calculation of stress is based on the equation

$$\sigma = \frac{F}{A} \tag{2}$$

where F is the load measured by the UTM and A is the area of the sample normal to the force applied by the machine. By calculating the stress and strain for each time step, a diagram can then be generated by putting

[1] Undergraduate student, Aerospace & Ocean Engineering Department.

stress over strain, allowing for the calculation of the relevant tension or compression modulus through the equation

$$E = \frac{\sigma}{\varepsilon} \tag{3}$$

Additionally, the UTM is capable of providing the load data on top of the aforementioned displacement and time data, enabling for the identification of maximum load experienced by the sample which further enables the calculation of the the mode I critical stress intensity factor $K_{IC}$ given by the equation

$$K_{IC} = \frac{P}{B\sqrt{W}} \times \frac{(2+\frac{a}{W})(0.886+4.64\frac{a}{W}-1\ .32\left(\frac{a}{W}\right)^2+14.72\left(\frac{a}{W}\right)^3-5.6(\frac{a}{W})^4)}{(1-\frac{a}{W})^{3/2}} \tag{4}$$

where P is the maximum load sustained by the sample, B is the thickness of the sample, W is the width of the sample, and a is the crack length for the sample (Borgoltz and Talluru, 2025).

Finally, using the Instron CEAST impact frame testing apparatus, a value for the measured energy absorbed by the sample fractured is tabulated and provided as data, which can then be compared to the theoretical fracture energy given by equation

$$E_f = E_0(1 - \frac{h_{mr}}{h_0}) \tag{5}$$

where $E_0$ is the potential energy of the hammer from the point which it is released from, $h_{mr}$ is the vertical position of the hammer at the maximum rise angle and $h_0$ is the vertical position of the hammer at the point from which the hammer is released (Borgoltz and Talluru, 2025).

Geometric measurements of the specimens were taken using calipers prior to testing to enable the calculation of stress and area-dependent properties. Potential limitations on this investigation include the use of mock materials that may not perfectly replicate behavior of PBXs exactly, the accuracy of dimensional measurements, and potential sample fabrication inconsistencies. These factors were considered during the analysis and interpretation of the results. Regardless of these potential limitations, the experimental procedure utilized allowed for meeting the core objectives. Specifically, this study effectively determined and compared the tensile and compressive moduli and strengths, quantified the mode I fracture toughness through compact tension testing, and measured the impact energy absorption via Charpy tests for both the neat and CNT nanoparticle reinforced material variants. These findings enabled a direct assessment of how CNT reinforcement influenced the key mechanical properties investigated.

The remainder of this report is organized such that the following section discusses the specific details of the equipment/apparatus used along with the procedure before leading into a section containing the results and uncertainties prior to concluding thoughts and summary.

## II. Apparatus and Techniques

### A. Instron Universal Testing Machine (UTM)

The tests for tension, compression, and fracture toughness necessary to meet the complete characterization of the samples were performed via the use of an Instron Model 5900 Universal Testing Machine or UTM. See Figure 2 for an image of the machine.

The UTM includes a stationary bottom fixture as well as a mobile top fixture capable of vertical movement. This top fixture is connected to a movable crosshead which is capable, through the use of dual jack screws, in providing precise movement. This also enables for the displacement or strain rate to be controlled and set as required by ASTM standards. For the investigation conducted, a constant crosshead displacement rate of 2 mm/min, equivalent to a strain rate of 0.12/min, was utilized for all tests performed on the UTM. The loading applied on the sample is calculated via the use of a 2580 series single-axis load cell which is capable of measuring a maximum loading of 50 kN to an accuracy of 5 N as per manufacturer specifications (Borgoltz and Talluru, 2025). Therefore, the primary uncertainty for load calculations will thus be 5 N. The crosshead track, while precise due to the aforementioned dual jack screws, also has a displacement resolution of 0.0001 mm and thus the primary uncertainty associated with the displacement readings can be considered as 0.0001 mm (Borgoltz and Talluru, 2025).

In order to collect the necessary time, displacement, and loading data discussed in the introduction for use in calculating values used for the objectives, the UTM posseses a real-time data acquisition system through a computer attached to the UTM running Bluehill Software. Results from the UTM are inherently limited by the load cell's accuracy of ±5 N, which would be significant for low-strength failure testing, and

the finite displacement resolution. Proper fixture selection for the tension, compression, or compact tension tests as well as secure mounting are necessary as well to ensure accurate results and avoid sample slippage, which could otherwise introduce errors into the stress-strain or load-displacement data.

### B. Instron CEAST 9050 Manual Impact Frame

The test for impact absorbing ability necessary to meet the characterization of the samples was performed via the use of an Instron CEAST 9050 manual impact frame. See Figure 3 for an image of the machine.

This apparatus calculated the energy absorbed by a notched specimen during fracture caused by a swinging pendulum hammer. The experiment utilized a Charpy hammer with length L of 326.8 mm where L is defined as the distance from the rotational center to the impact point (Borgoltz et al., 2025). The CEAST 9050 has a internal computer and touch screen interface that measured the maximum rise angle with a resolution of 0.1 degrees (thus providing a primary uncertainty for the angle reading of 0.1 degrees) (Borgoltz and Talluru, 2025). This computer also calculates the energy absorption of the sample with a resolution of 0.001 J providing the primary uncertainty of 0.001 J for the measured energy reading (Borgoltz and Talluru, 2025).

This energy reading accounts for the losses caused by friction and other external factors due to a calibration step performed on the machine prior to the official testing, allowing a more accurate result than the theoretical calculations outlined through Equation 5. Also necessary for accuracy for the final measurement is the positioning of the sample, which is made easier via the use of a prefabricated v-notch present in the sample, as shown in Figure 1. This notch allows for a centering pin on the mounting anvil of the machine to be placed into the notch and precisely position the sample. However, limitations still exist due to the notch quality and placement. Using an initial potential energy of 5.40 J and release angle of 150 degrees, which is given by the manufacturer, the theoretical value for the fracture energy can be then compared with the measured value to meet the 4$^{th}$ objective (Borgoltz and Talluru, 2025).

### C. Procedure Overview

The procedure utilized to perform the complete characterization of the mechanical properties of the two material variant samples involved the measurement of sample dimensions, impact energy testing, along with compression, tension, and compact tension testing.

Prior to mechanical loading, all of the different sample geometries and variants were measured thrice using digital calipers for the dimensions needed for use in the relevant tests' equations. Specifically, for the compression sample, the height of the circular cylinder shaped sample (see Figure 1 for reference) was measured alongside the diameter to calculate the value of $l_0$ used for strain and A used for stress. Similarly, for the tension sample, the gauge length was measured for the value of $l_0$ alongside the width and thickness of the gauge section for the value of A. For the compact tension test, the thickness beneath the notch was measured alongside the actual thickness of the sample as the pre-crack length of the samples were provided. The measurement of the impact testing samples was not necessary but performed for completeness on the length, height, and width of the sample.

Following measurement of dimensions, the compression testing began involving the setup of the UTM for compression specifications set by ASTM D695 (Sengezer et al., 2025). In order to setup specifically for compression, compression testing plates are installed and secured via the use of pins. These are the top and bottom interchangeable fixtures aforementioned in the description of the UTM. Following the installation of the fixtures, the displacement values are zeroed in order to allow for accurate measured values in the data. Following these setup steps, the Seidel Compression method is run until automatically stopped after ensuring the displacement rate is set to 2 mm/min. After the compression testing, the specific respective fixtures for tension and compact tension testing are installed prior to zeroing the displacement values and performing the Seidel Tension or Seidel Compact Tension tests for the tension and compact tension tests respectively.

Concurrently to the tensile test running on the UTM, Charpy impact testing was conducted using the Instron CEAST 9050 manual impact frame. After turning on the impact frame's internal computer, the calibration needed to calculate the frictional losses is performed through the release of the hammer and 12 cycles of the hammer swinging (Borgoltz et al., 2025). Following calibration, the impact testing frame is

reset by returning the hammer to the initial height behind the locking pin followed by loading the Thin Sample parameter set via the test selection menu on the internal computer. After ensuring safety protocols were followed and that calibration was completed, one notched Charpy sample of one material variant was placed on the mounting anvil. The sample was aligned using the centering pin, as discussed in the impact frame apparatus discussion, which was then lowered to avoid collision with the hammer. The 5.4 J pendulum hammer was released from its 150-degree starting position and upon fracture of the sample, the hammer's swing was stopped using the brake knob. The absorbed impact energy thus was directly read and recorded from the "Test Results" screen and the following material variant was setup in a repeated procedure and tested.

All digitally recorded data from the UTM and the direct energy readings from the Charpy tester were saved for analysis.

## III. Results and Discussion

### A. Strain versus Stress for Tension and Compression Tests

Using the procedure for compression and tension testing allowed for the generation of time, displacement and loading data which could then be used alongside measured dimensions on Equation 1 and Equation 2 to generate corresponding stress and strain data. From this data, using code shown in Figure 4, Plot 1 and Plot 2 were plotted to depict the stress versus strain plots for compression and tension testing respectively.

**Plot 1. Stress versus Strain for Compressive Loading of mock PBX samples.**

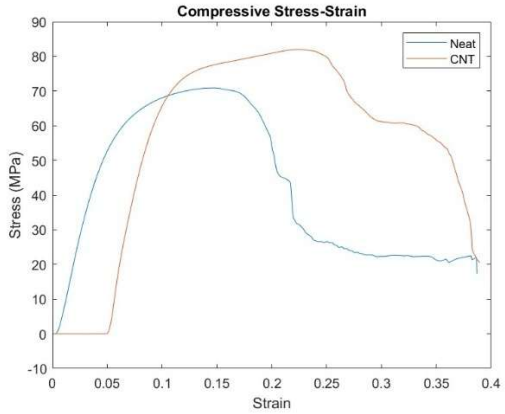


**Plot 2. Stress versus Strain for Tensile Loading of mock PBX samples.**

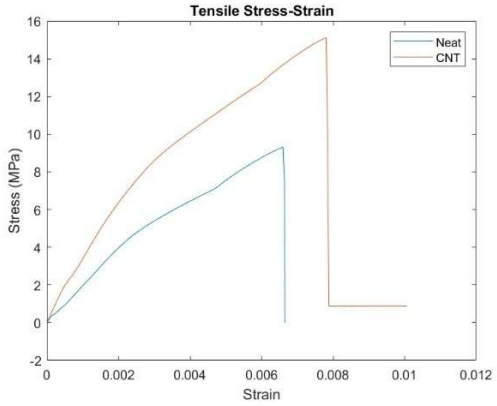

The results show that the sample with CNT nanoparticles reinforcements for both cases of tensile and compressive loading is capable of handling a greater strain prior to yielding/fracturing as the CNT curve is reaching a higher absolute stress and is shifted further to the right demonstrating a greater capability to withstand loading and not yield against higher stresses. From the MATLAB plots, values for the peaks of the stress strain curve can be compared to the starting points of the stress strain curve as shown in Table 1. Using these values, a linear approximation of the slope can be performed in order to calculate the compressive/tensile modulus via the relationship shown in Equation 3, resulting in values for tensile/compressive strength, tensile/compressive strain, and tensile/compressive modulus as shown in Table 2.

**Table 1. Relevant points for tensile/compressive strength, tensile/compressive strain, and tensile/compressive modulus.**

| | Tensile Max Stress | Tensile Min Stress | Tensile Max Strain | Tensile Min Strain | Compress Max Stress | Compress Min Stress | Compress Max Strain | Compress Min Strain |
|---|---|---|---|---|---|---|---|---|
| Neat | 9.32111 | 0.0875 | 0.0066 | 0.00003 | 62.6831 | 0.0000 | 0.1171 | 0.0000 |
| CNT | 15.1128 | 0.0875 | 0.0078 | 0.00003 | 73.0532 | 0.0000 | 0.0725 | 0.0455/0 |
| Units | MPa | MPa | N/A | N/A | MPa | MPa | N/A | N/A |

**Table 2. Tensile/compressive strength, tensile/compressive strain, and tensile/compressive modulus.**

| | Tensile Strength | Tensile Strain | Tensile Modulus | Compressive Strength | Compressive Strain | Compressive Modulus |
|---|---|---|---|---|---|---|
| Neat | 9.32111 | 0.0066 | 1405.420 | 62.6831 | 0.1171 | 535.295473954 |
| CNT | 15.1128 | 0.0078 | 1933.758 | 73.0532 | 0.0725 | 2705.6740/1007.6303 |
| Units | MPa | N/A | MPa | MPa | N/A | MPa |

The results from these tabulations further demonstrate that the presence of CNT nanoparticles create a reinforcement effect in the mock PBXs as the compressive and tensile strengths are higher along with the modulus being significantly greater. Notably, the compressive modulus for the CNT sample versus the neat sample sees almost a 5x increase. This is likely to be a result of errors which is hinted at through Plot 1 as the stress on the PBX sample does not increase from 0 until reaching 0.0455 on the strain (as underlined in Table 1.) By changing the value of this likely erroneous value into 0, a CNT compressive modulus of 1007.6303 MPA is calculated which is more reasonable. Changing the value to zero would also match the expected result of a minimum strain value for which stress becomes non-zero being very near 0 as is seen in the neat sample undergoing compression as well as both samples varieties undergoing tension.

Overall uncertainties (see Appendix A) show that the tensile stress (i.e tensile strength) has an uncertainty of only 0.111 MPa while tensile strain has an uncertainty of only 0.000113 and compressive stress (i.e compressive strength) has an uncertainty of only 0.7514117885 MPa while compressive strain has an uncertainty of only 0.00259. Since these are, relative to the respective actual values, fairly small, the calculations performed can be taken with a degree of confidence and should match expected physical behaviors.

### B. Impact Testing Material Comparisons

Using the procedure for impact energy testing allowed for the measured value of absorbed energy by the Instron CEAST 9050 Manual Impact Frame, for which results are shown in Table 3 extracted from Figure 5.

**Table 3. Tensile/compressive strength, tensile/compressive strain, and tensile/compressive modulus.**

| | *Absorbed Energy (%)* | *Impact Velocity* | *Absorbed Energy (J)* | *Rise Angle* |
|---|---|---|---|---|
| Neat | 3.94% | 3.55 m/s | 0.212 | -141.650 |
| CNT | 4.64% | 3.55 m/s | 0.251 | -140.800 |

The result from these measured absorbed energies demonstrate a greater capability of the CNT sample in absorbing energy resulting in a greater energy requirement to cause fracturing that that of a sample with CNT. In a physical sense, this means that causing a CNT reinforced sample of PBX to fracture would be more difficult than causing a regular sample of PBX to fracture. The rise angle matches expectations as, due to the greater amount of energy absorbed from the pendulum hammer by the CNT sample, less energy is available causing the height and thus angle after impact for the CNT sample being lower than that of the neat sample. Furthermore, comparisons can also be made to the theoretical values for fracture energy through the use of Equation 5, where $h_{mr}$ and $h_0$ can be calculated from the length L of the hammer described in the apparatus section as 326.8 via the equations

$$h_{mr} = L(1 - \cos(\theta_{rise})) \tag{6}$$

and

$$h_0 = L(1 - \cos(\theta_0)) \tag{7}$$

where $\theta_{rise}$ is the rise angle from Table 3 and $\theta_0$ is the initial angle of the hammer which is given in apparatus section as 150 degrees. Using these intermediate values in the Equation 5 yields

**Table 5. Compact tension testing peak loads.**

| | *Absorbed Energy (J)* | *Initial height (m)* | *Hammer rise height (m)* | *Absorbed Energy Theory (J)* |
|---|---|---|---|---|
| Neat | 0.212 | 0.609817 | 0.583088 | 0.236689 |
| CNT | 0.251 | 0.609817 | 0.580052 | 0.263575 |

The result from this table demonstrates that the Instron CEAST 9050 Manual Impact Frame's calibration step is capable of isolating and taking into account the frictional and environmental factors that also lead to a reduction in energy aside from just the fracturing of the samples as the data shows that theory predicted a slightly greater value of energy being absorbed that truly was by the sample as some of the energy was absorbed not by the sample but by the friction of the hammer swinging and the air resistance against the hammer. Overall, the results of the impact energy testing demonstrate a greater ability of the CNT sample in absorbing loads and a validation of the apparatus used to calculate said absorbed energy.

### C. Fracture Toughness/$K_{IC}$ Comparison

Using the procedure for compact tension testing allowed for the automatic outputting of peak loads by the UTM, as shown in Table 5.

**Table 5. Compact tension testing peak loads.**

| | *Peak Load (N)* |
|---|---|
| Neat Sample #1 | 417.05 |
| Neat Sample #2 | 333.79 |
| CNT Sample #1 | 467.07 |
| CNT Sample #2 | 470.65 |

The result from these measured peak forces demonstrates that the use of nanoparticle reinforcements through CNT in the samples allows for increased resistance to compact tension, thus improving the strength characteristics of the material. Table 5 is visualized through Plot 3 shown below.

**Plot 3. Peak Loading for Neat Versus CNT Samples.**

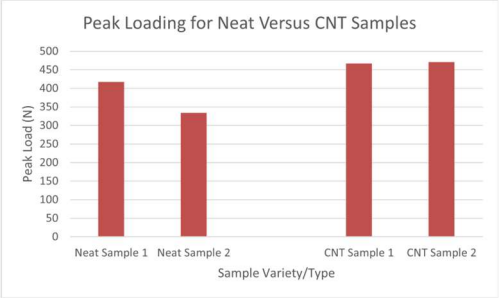


The procedure for the compact tension testing also outputted the time, displacement and loading data that was outputted in the Section III, Part A due to the use of the same apparatus, the UTM. As a result, a graph of the force versus displacement can also be made to visualize the fracture moment by identifying the point at which the force peaks and then drops to zero even as displacement continues. Furthermore, using the peak loading forces tabulated previously along with the average width, thickness, and crack length of the sample in Equation 4 gives an average $K_{IC}$ value of 2276 MPa/sqrt(m) for the CNT samples and an average $K_{IC}$ value of 1823 MPa/sqrt(m) for the neat samples as shown in Plot 4 generated from code shown in Figure 6. From these calculated $K_{IC}$ values, using the equation

$$Percent\ Increase = \frac{new-original}{original} \times 100 \tag{8}$$

where new is the improved or enhanced value (in our case the $K_{IC}$ for CNT) while old is the original value ($K_{IC}$ for neat) allows for the calculation of the enhancement in fracture toughness. Using the $K_{IC}$ values calculated and shown in Plot 4 gives the percent enhancement of the fracture toughness as 25% which demonstrates that using CNT nanoparticles for reinforcement further increases another material characteristic of PBX samples.

**Plot 4. Peak Loading for Neat Versus CNT Samples.**

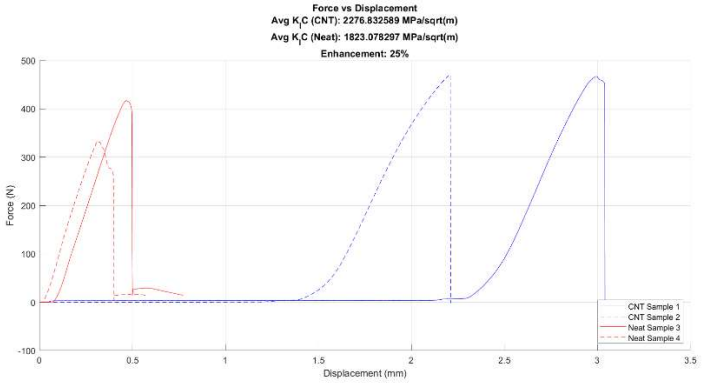


As a result of the compact tension testing, a clear result is obtained on the significantly improved resistance to compact tension and improvement in fracture toughness caused by the use of CNT nanoparticles in samples of PBX due to the 25% enhancement in $K_{IC}$ for samples using CNT over those without and due to the improved peak loading the CNT samples are capable of withstanding.

Plot 4 also demonstrates a level of uncertainty in the obtained results due to the need for averages as a result of differences in the peak loading values which have a direct impact on the $K_{IC}$ values calculated. From Appendix A, the uncertainty in the fracture toughness measurement can be calculated and is found to be only 0.0210 MPa/sqrt(m), which shows a great degree of accuracy in terms of the actual value calculated due to the relative size of the actual value compared to the uncertainty. As a result, the calculation for $K_{IC}$ can be taken with a great deal of confidence.

## IV. Conclusion

An experiment has been performed to determine the complete material and mechanical

characteristics of mock polymer bonded explosives (PBX) samples. Two material variants were tested, a "neat" type material with only epoxy and ammonium perchlorate (AP) along with a "CNT" type reinforced with its namesake, carbon nanotubes. Standardized mechanical tests including tension, compression, compact tension/fracture toughness, and impact energy tests were performed using an Instron Universal Testing Machine (UTM) and an Instron CEAST 9050 Manual Impact Frame. Data acquired from these tests allowed for the calculation of characteristics such as the tensile/compressive strength, tensile/compressive strain, tensile/compressive modulus, mode I fracture toughness ($K_{IC}$), and impact energy absorption between the neat and CNT nanoparticle reinforced samples. The following conclusions were drawn.

1. The addition of just 1% CNT nanoparticles by weight significantly increased both the tensile and compressive strengths of the mock PBX material compared to the neat samples. Similarly, the tensile modulus and compressive modulus also increased substantially although potential data artifacts were taken into account for the results.
2. Compact tension testing revealed that the CNT nanoparticle reinforced samples have a greater resistance to fracturing with the calculated mode I fracture toughness being enhanced by approximately 25% compared to the neat samples' mode I fracture toughness.
3. The impact energy testing further demonstrated that the CNT nanoparticle reinforced samples absorbed more energy during fracture compared to the neat samples, indicating a greater ability to resist fracturing due to the greater energy requirement needed to cause fracturing.
4. Comparison between measured absorbed energy in impact testing and theoretical calculations for said absorbed energy suggested that the testing apparatus effectively accounted for system energy losses like friction and environmental factors by measuring energy absorption values slightly lower than theory predicts for ideal cases as expected.
5. Across all mechanical tests performed, the presence of CNT nanoparticles consistently led to measurable improvements in the mechanical performance of the mock PBX material and using CNT nanoparticles for reinforcement is a effective and viable method of improving the material properties of PBX in use cases like for solid rocket propellants.

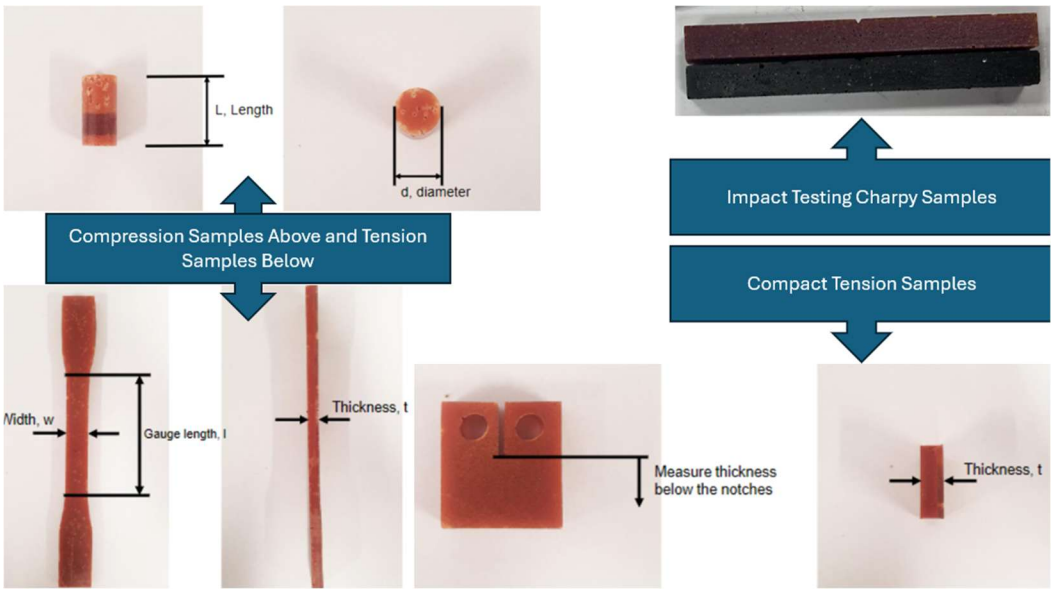


**Fig. 1. Examples of Varying Samples and Sample Geometries/Dimensions. Adapted from A. Borgoltz and V. Talluru (2025).**

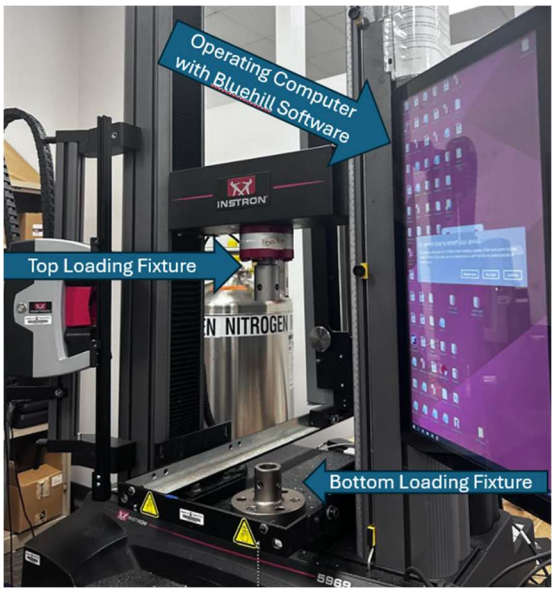


**Fig. 2. Instron Universal Testing Machine**

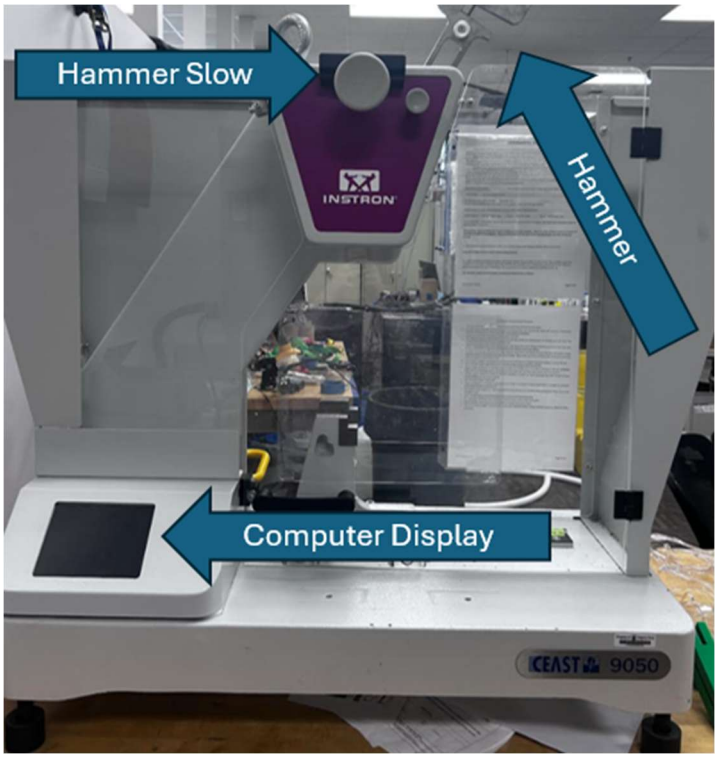


**Fig. 3. Instron CEAST 9050 Manual Impact Frame**

```
clear; close all; clc;

%all in mm or mm^2
L0_ten_cnt = 88.08;
L0_ten_neat = 85.49;
L0_comp_cnt = 24.15;
L0_comp_neat = 24.92666667;
A0_compneat = 129.7542; %in mm^2
A0_compcnt = 132.80037;
A0_tenneat = 80.99777778; %in mm^2
A0_tencnt = 65.03542222;

data_neat_ten = readmatrix('tenneat.csv', 'NumHeaderLines', 4);
data_cnt_ten = readmatrix('tencnt.csv', 'NumHeaderLines', 4);
strain_neat_ten = data_neat_ten(:,2) / L0_ten_neat;
stress_neat_ten = data_neat_ten(:,3) / A0_tenneat;
strain_cnt_ten = data_cnt_ten(:,2) / L0_ten_cnt;
stress_cnt_ten = data_cnt_ten(:,3) / A0_tencnt;

data_neat_comp = readmatrix('compneat.csv', 'NumHeaderLines', 4);
data_cnt_comp = readmatrix('compcnt.csv', 'NumHeaderLines', 4);
strain_neat_comp = data_neat_comp(:,2) / L0_comp_neat;
stress_neat_comp = data_neat_comp(:,3) / A0_compneat;
strain_cnt_comp = data_cnt_comp(:,2) / L0_comp_cnt;
stress_cnt_comp = data_cnt_comp(:,3) / A0_compcnt;

figure;
plot(strain_neat_ten, stress_neat_ten);
hold on;
plot(strain_cnt_ten, stress_cnt_ten);
xlabel('Strain'); ylabel('Stress (MPa)');
title('Tensile Stress-Strain');
legend('Neat','CNT');

figure;
plot(strain_neat_comp, stress_neat_comp);
hold on;
plot(strain_cnt_comp, stress_cnt_comp);
xlabel('Strain'); ylabel('Stress (MPa)');
title('Compressive Stress-Strain');
legend('Neat','CNT');
```

**Fig. 4. Stress Versus Strain Plot Code**

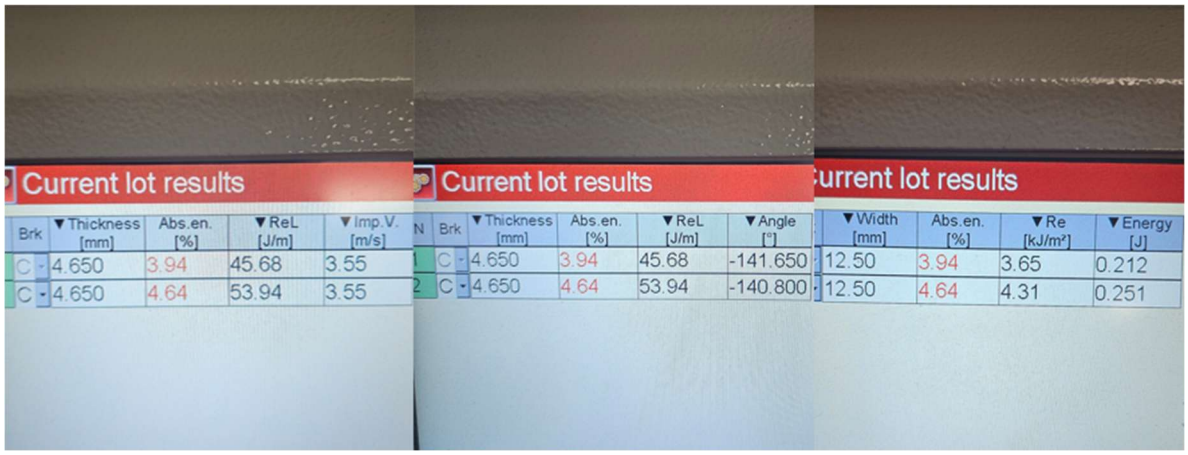


**Fig. 5. Results from Charpy Impact Energy Test with Impact Velocity, Rise Angle, and Energy Absorbed (in J and %).**

```
W_m = 25 / 1000;
a_m = (9 + 1.5) / 1000;
B_m = 10 / 1000;

Pmax_kN = [467.07, 470.65, 417.05, 333.79] / 1000;

data_file_1 = readtable('Facture Combined_1_2.csv');
data_file_2 = readtable('Facture Combined_2_2.csv');
data_file_3 = readtable('Facture Combined_3_2.csv');
data_file_4 = readtable('Facture Combined_4_2.csv');

x = a_m / W_m;
fx = (2 + x) * (0.886 + 4.64*x - 13.32*x^2 + 14.72*x^3 - 5.6*x^4) / (1 - x)^(3/2);
K_IC = (Pmax_kN / (B_m * W_m^(1/2))) * fx;

K_IC_CNT_avg = mean(K_IC(1:2));
K_IC_Neat_avg = mean(K_IC(3:4));
percent_enhancement = ((K_IC_CNT_avg - K_IC_Neat_avg) / K_IC_Neat_avg) * 100;

figure; hold on;
plot(data_file_1.Displacement, data_file_1.Force, 'b-', 'DisplayName', 'CNT Sample 1');
plot(data_file_2.Displacement, data_file_2.Force, 'b--', 'DisplayName', 'CNT Sample 2');
plot(data_file_3.Displacement, data_file_3.Force, 'r-', 'DisplayName', 'Neat Sample 3');
plot(data_file_4.Displacement, data_file_4.Force, 'r--', 'DisplayName', 'Neat Sample 4');

xlabel('Displacement (mm)');
ylabel('Force (N)');
title_str = sprintf('Force vs Displacement\nAvg K_IC (CNT): %f MPa/sqrt(m)\nAvg K_IC (Neat): %f MPa/sqrt(m)\nEnhancement: %f%%', ...
    K_IC_CNT_avg, K_IC_Neat_avg, percent_enhancement);
title(title_str);

legend('Location', 'southeast');
grid on;
hold off;
```

**Fig. 6. Compact Tension Testing Code for Calculating $K_{IC}$ along with Loading vs Displacement.**

## REFERENCES


Borgoltz A., O'Donnel J., and Seidel G., 2025, AOE 3054 *Appendix 4 – Impact Strength Testing*, A.O.E. Department, Virginia Tech, Blacksburg, VA. Last modified April 1, 2025.

Borgoltz A. and Talluru V., 2025, *Experiment 5 – Operational Procedures*, A.O.E. Department, Virginia Tech, Blacksburg, VA. Last updated April 15, 2025.

Sengezer E., Borgoltz A., Shirodkar N., and Seidel G., 2025, *Experiment 5 – Materials Testing*, A.O.E. Department, Virginia Tech, Blacksburg, VA. Last modified April 1, 2025.


## Appendix A

### A. Uncertainty Analysis

The uncertainties for measurements made during the investigation were calculated for 20:1 odds and include the resolution of Instron equipment such as the resolution for which the crosshead could be displaced, the resolution to which the load could be measured, and the resolution for which the impact energy could be displayed for impact testing. Uncertainty calculations utilized the root sum square equation,

$$\delta(R) = \sqrt{\left(\frac{\partial R}{\partial a}\delta(a)\right)^2 + \left(\frac{\partial R}{\partial b}\delta(b)\right)^2 + \left(\frac{\partial R}{\partial c}\delta(c)\right)^2 + \cdots} \tag{9}$$

where a, b, c… are the primary measurements that the measurement of R depends on. These calculations were performed via a spreadsheet table which has been given in Tables 6 through 10 for uncertainties in tensile stress, tensile strain, fracture toughness, compressive stress, and compressive strain.

**Table 6. Uncertainty in Tensile Stress.**

| | **Primary Measurements** | | | Perturbation | |
|---|---|---|---|---|---|
| | | Quantity | Uncertainty | a+da, b | a,b+db |
| a | Force (N) | 754 | 5 | 759 | 754 |
| b | Cross-Sectional Area (m^2) | 8.10E-05 | 8.10E-07 | 8.09978E-05 | 8.18078E-05 |
| | | | | | |
| | **Final Results** | | | | |
| | Stress (pa) | 9.31E+06 | | 9370627.452 | 9216730.063 |
| | | | Change | 61730.08862 | -92167.30063 |
| | **Total Uncertainty (pa)** | 110929.7757 | | | |

**Table 7. Uncertainty in Tensile Strain.**

| | **Primary Measurements** | | | Perturbation | |
|---|---|---|---|---|---|
| | | Quantity | Uncertainty | a+da, b | a,b+db |
| a | Displacement (mm) | 0.5677 | 0.0005677 | 0.5682677 | 0.5677 |
| b | Average Gauge Length (mm) | 5.00E+01 | 5.00E-01 | 50 | 50.5 |
| | | | | | |
| | **Final Results** | | | | |
| | Strain | 1.14E-02 | | 0.011365354 | 0.011241584 |
| | | | Change | 1.1354E-05 | -0.000112416 |
| | **Total Uncertainty** | 0.000112988 | | | |

**Table 8. Uncertainty in Fracture Toughness.**

| | **Primary Measurements** | | | Perturbation | | |
|---|---|---|---|---|---|---|
| | | Quantity | Uncertainty | a+da, b, c | a,b+db, c | a,b, c+dc |
| a | Peak Load (N) | 468.5 | 5 | 473.5 | 468.5 | 5 |
| b | Thickness(m) | 1.22E-02 | 1.22E-04 | 0.01218 | 0.0123018 | 0.0123018 |
| c | Width(m) | 1.28E-02 | 1.28E-04 | 1.28E-02 | 1.28E-02 | 1.29E-02 |
| | Crack Length(m) | 0.0023 | 0 | | | |
| | | | | | | |
| | **Final Results** | | | | | |
| | Energy | 1.37E+06 | | 1382210.157 | 1354073.747 | 1360827.3 |
| | | | Change | 14595.67219 | -13540.73747 | -6.79E+03 |
| | **Total Uncertainty** | 21034.52983 | | | | |

**Table 9. Uncertainty in Compressive Stress.**

| | **Primary Measurements** | | | Perturbation | |
|---|---|---|---|---|---|
| | | Quantity | Uncertainty | a+da, b | a,b+db |
| a | Force (N) | 10065.8955 | 5 | 10070.8955 | 10065.8955 |
| b | Cross-Sectional Area (m^2) | 1.33E-04 | 1.33E-06 | 0.0001328 | 0.000134128 |
| | | | | | |
| | **Final Results** | | | | |
| | Stress (pa) | 7.58E+07 | | 75834911.42 | 75046792.96 |
| | | | Change | 37650.53039 | -750467.9296 |
| | **Total Uncertainty (pa)** | 751411.7885 | | | |

**Table 10. Uncertainty in Compressive Stress.**

| | **Primary Measurements** | | | Perturbation | |
|---|---|---|---|---|---|
| | | Quantity | Uncertainty | a+da, b | a,b+db |
| a | Displacement (mm) | 6.2652 | 0.0062652 | 6.2714652 | 6.2652 |
| b | Average Gauge Length (mm) | 2.42E+01 | 2.42E-01 | 24.15 | 24.3915 |
| | | | | | |
| | **Final Results** | | | | |
| | Strain | 2.59E-01 | | 0.259688 | 0.256859972 |
| | | | Change | 0.000259429 | -0.0025686 |
| | **Total Uncertainty** | 0.002581668 | | | |